Cell Tissue Res (2006) 324: 267–277
DOI 10.1007/s00441-005-0142-8

REGULAR ARTICLE

Manfred Infanger · Peter Kossmehl · Mehdi Shakibaei · Johann Bauer · Stephanie Kossmehl-Zorn · Augusto Cogoli · Francesco Curcio · Alexander Oksche · Markus Wehland · Reinhold Kreutz · Martin Paul · Daniela Grimm

Simulated weightlessness changes the cytoskeleton and extracellular matrix proteins in papillary thyroid carcinoma cells

Received: 31 May 2005 / Accepted: 23 November 2005 / Published online: 24 January 2006

Abstract Studies of astronauts, experimental animals, and cells have shown that, after spaceflights, the function of the thyroid is altered by low-gravity conditions. The objective of this study was to investigate the cytoskeleton and extracellular matrix (ECM) protein synthesis of papillary thyroid cancer cells grown under zero *g*. We investigated alterations of ONCO-DG 1 cells exposed to simulated microgravity on a three-dimensional random-positioning machine (clinostat) for 30 min, 24 h, 48 h, 72 h, and 120 h (n=6, each group). ONCO-DG 1 cells grown under microgravity exhibited early alterations of the cytoskeleton and formed multicellular spheroids. The cytoskeleton was disintegrated, and nuclei showed morphological signs of apoptosis after 30 min. At this time, vimentin was increased. Vimentin and cytokeratin were highly disorganized, and microtubules (α–tubulin) did not display their typical radial array. After 48 h, the cytoskeletal changes were nearly reversed. The formation of multicellular spheroids continued. In parallel, the accumulation of ECM components, such as collagen types I and III, fibronectin, chondroitin sulfate, osteopontin, and CD44, increased. The levels of both transforming growth factor beta-1 (TGF-β_1) and TGF-β receptor type II proteins were elevated from 24 h until 120 h clinorotation. Gene expression of TGF-β_1 was clearly enhanced during culture under zero *g*. The amount of E-cadherin was enhanced time-dependently. We suggest that simulated weightlessness rapidly affects the cytoskeleton of papillary thyroid carcinoma cells and increases the amount of ECM proteins in a time-dependent manner.

Keywords Extracellular matrix proteins · Cytoskeleton · Weightlessness · Papillary thyroid carcinoma · Cell culture (Human)

The work of Augusto Cogoli was supported by ETH Zurich, Switzerland.

M. Infanger
Department of Trauma and Reconstructive Surgery,
Charité University Medical School, Center of Space Medicine,
Benjamin Franklin Medical Center,
12200 Berlin, Germany

P. Kossmehl · S. Kossmehl-Zorn · M. Wehland · R. Kreutz · M. Paul · D. Grimm (✉)
Institute of Clinical Pharmacology and Toxicology,
Charité University Medical School, Center of Space Medicine,
Campus Benjamin Franklin,
14195 Berlin, Germany
e-mail: daniela.grimm@charite.de
Tel.: +49-30-8445-1707
Fax: +49-30-8445-1762

M. Shakibaei
Institute of Anatomy, Charité University Medical School,
Campus Benjamin Franklin,
14195 Berlin, Germany

M. Shakibaei
Institute of Anatomy, Ludwig Maximilian University,
80336 Munich, Germany

J. Bauer
Max Planck Institute of Biochemistry,
82152 Martinsried, Germany

A. Cogoli
Space Biology Group,
Technopark, ETH Zurich,
8005 Zurich, Switzerland

F. Curcio
Department of Pathology, University of Udine,
33100 Udine, Italy

A. Oksche
Institute of Pharmacology, Charité University Medical School,
Campus Benjamin Franklin,
14195 Berlin, Germany

Introduction

Eukaryotic cells are highly sensitive to mechanical forces, as the location of cellular components depends on the integrity and spatial organization of the cytoskeletal architecture (microtubules, microfilaments, and intermediate filaments) and the nucleoskeleton. The organization of these cellular compartments and signal proteins is regulated by extracellular signals, viz., cell-cell and cell-extracellular matrix

(ECM) signaling (Lelievre et al. 1998; Roskelley et al. 1994). The ECM enwraps cells, acts as a mechanical scaffold, and influences proliferation, differentiation, adhesion, migration, gene expression, and tissue integrity (Adams and Watt 1993; Hagios et al. 1998). Its structural molecules comprise various collagens, fibronectin, vitronectin, tenascin, elastin, fibrillin, and proteoglycans (Merker 1994). Major basement-membrane molecules are laminin, type IV collagen, and nidogen (Yurchenco and O'Rear 1994).

Previous studies have shown that microgravity (1) influences cellular functions, such as hormone metabolism, differentiation, and growth (Cogoli 1992; Grimm et al. 2002; Margolis et al. 1999; Martin et al. 2000), (2) causes changes in the composition of the ECM, and (3) induces apoptosis (Kossmehl et al. 2003; Maccarrone et al. 2003). Moreover, weightlessness affects the cytoskeleton of several types of cells, such as osteoblasts (Hughes-Fulford and Lewis 1996), lymphocytes (Lewis et al. 1998, 2001; Schatten et al. 2001), glial cells (Uva et al. 2002), and breast cancer cells (Vassy et al. 2001). The cellular alterations appear to be responsible for the observations made in astronauts and experimental animals during and after a stay in orbit. The function of many organs and systems under low gravity undergo physiological changes, such as loss of fluids and electrolytes, osteoporosis, loss of muscle mass, reduced immune response, orthostatic intolerance, cardiac atrophy, arrhythmias, disruption of the biological clock, sleep loss, and others (Nicogossian et al. 1989; White and Averner 2001).

Many effects of weightlessness can be observed when microgravity is mimicked by a three-dimensional clinostat (random-positioning machine), averaging the exposure of the biological object to the earth gravity vector by random rotation. Using clinorotation for 5 days, we have evaluated the effects of simulated microgravity on the human papillary thyroid carcinoma cell line, ONCO-DG 1, which is tumorigenic in nude mice and capable of forming spheroids (Grimm et al. 1992, 1997). We have investigated the role of gravity in signal transduction across the cytoskeleton to the nucleus and changes of ECM proteins during long-term clinorotation of papillary thyroid carcinoma cells.

Materials and methods

Random-positioning machine

The random-positioning machine (also referred to as a three-dimensional clinostat) simulates low-gravity conditions (microgravity). It was developed by T. Hoson in Japan (Hoson et al. 1992) and is manufactured by Dutch Space (formerly Fokker Space, Leiden, The Netherlands). The machine is composed of an inner and an outer frame with a platform in the middle to accommodate the samples. The frames rotate independently of each other in random directions. Gravimeters fixed to the frames indicate the gravity vectors during rotation. On the random-positioning machine, the samples are fixed as close as possible to the center of the inner rotating frame. This frame rotates within another rotating frame. Both frames are driven by separate motors. The rotation of each frame is randomly and autonomously regulated by computer software. The random-positioning machine can be operated as a random-walk three-dimensional clinostat (basic mode), as a two-dimensional clinostat, or as a centrifuge.

The random-positioning machine was located in a room with a controlled temperature (37±1°C). The angular velocity of rotation was selected as 60°/s. Maximum weight of loading was 20 kg. Maximum power for experiments was 24 W.

Cell culture procedure

To start a culture, we used a syringe to fill culture flasks with complete medium, taking care to avoid air bubbles. The filled culture flasks were screwed onto the clinostat operated under the conditions given above for rotation times of 30 min, 24 h, 48 h, 72 h, and 120 h. We used ONCO-DG 1 cells at passage 40 for the experiments. Sixty subconfluent monolayers (5×10^6 cells/flask) were randomized to the various study groups: 30 ground controls (30 min, 24 h, 48 h, 72 h, 120 h; n=6 for each group) and 30 samples for the clinorotation experiments (30 min, 24 h, 48 h, 72 h, 120 h; n=6 for each group). Ground controls were static control cultures kept in the same room as the random-positioning machine.

In addition, we used the CGTH-W-1 cell line (DSMZ no. ACC 360, Braunschweig, Germany) to examine the amount of cells positive for osteopontin (OPN) and CD44. The CGTH-W-1 cell line is a human thyroid carcinoma established from the sternal metastasis of a follicular thyroid carcinoma removed from a 70-year-old Chinese woman in 1993 (Lin et al. 1996). Six static ground controls (1 g) and 18 samples for clinorotation (zero g: 4 h, 24 h, and 72 h; n=6 each group) were investigated.

Cell culturing

ONCO-DG 1 cells (passage 40) were cultured in RPMI 1640 medium containing 100 μM sodium pyruvate and 2 mM L-glutamine and supplemented with 10% fetal calf serum, 100 U/ml penicillin, and 100 μg/ml streptomycin (Invitrogen, Eggenstein, Germany) until subconfluency (Grimm et al. 1992). Complete medium was changed every day.

Cells from the CGTH-W-1 line were cultured in 90% RPMI 1640 and 10% fetal calf serum until subconfluency. Complete medium was changed every day.

Cytoskeletal evaluations

The morphology of the microtubule cytoskeleton (alpha-tubulin) and intermediate filaments (cytokeratin, vimentin) was evaluated by indirect immunofluorescence. Static control cells and cells cultured under zero g, all grown on supercell chamber slides (BD Biosciences, Heidelberg, Germany), were washed twice in phosphate-buffered saline

(PBS) and fixed in ethanol/methanol solution (2:1) at room temperature for 30 min. For immunofluorescence staining, the cells were washed twice in PBS, incubated with the first antibody against alpha-tubulin, vimentin, or pan-cytokeratin (Sigma, Taufkirchen, Germany) for 24 h at room temperature, rinsed in PBS, incubated for 24 h with anti-mouse fluorescein isothiocyanate (FITC)-conjugated immunoglobulin antibody (DAKO, Hamburg, Germany), washed in PBS, incubated with propidium iodide (Molecular Probes, Eugene, Ore., USA) for 1 h at 37°C, rinsed again in PBS, mounted with Vectarshield immunofluorescence mounting medium (Vector, Burlingame, Calif., USA), and sealed with nail polish. Microtubule and intermediate filament morphology was visualized by using a Zeiss laser-scanning confocal microscopy system. Propidium iodide staining was observed concurrently.

Acridine orange/ethidium bromide and 4′, 6-diamidino-2-phenylindole staining

The monolayers remaining under 1 *g* conditions at the bottom of the plastic culture flasks (BD Biosciences) and multicellular spheroids (MCS) formed during 24 h clinorotating were examined by phase-contrast microscopy. After culture, control and microgravity-exposed cells were stained with acridine orange/ethidium bromide (Molecular Probes) according to the method of Zhou et al. (1997).

Cells for 4′,6-diamidino-2-phenylindole (DAPI) staining were fixed with 4% formaldehyde and incubated in DAPI-containing medium (Molecular Probes). Stained nuclei were investigated by using fluorescence microscopy.

Image analysis

Altered cells and nuclei were quantitatively assessed by means of a video camera combined with a separate video control system (Sony MC-3255, AVT-Horn, Germany) adapted for a Zeiss Axiophot microscope. Image analysis was performed with freely available software (Image 1.62a, Scion) on a Power Macintosh 8200/120 computer with magnification at ×10. Details and application of the method were as described previously (Kossmehl et al. 2003).

Immunocytochemistry

For immunocytochemical staining, cells and MCS were seeded into one compartment of a four-chamber supercell chamber slide (BD Biosciences) and were incubated for 30 min (adhesion time). Subsequently, the monolayer cultures were washed twice in PBS, fixed with methanol and ethanol (1:2, room temperature, 30 min), and treated with the first antibody. The monoclonal antibody used for this study was directed against fibronectin (Sigma). Antigen-antibody complexes were visualized with the indirect immunoperoxidase technique as previously described (Grimm et al. 2001).

Microscopy

Cells grown in plastic culture flasks (BD Biosciences) and MCS were examined by phase-contrast microscopy (Olympus, Hamburg, Germany). Specimens were analyzed with a Zeiss 510 META inverted confocal laser-scanning microscope equipped with a Plan-Apochromat 63×/1.4 objective. Excitation and emission wavelengths were: λ_{exc}=364 nm and λ_{em}=>475 nm for DAPI and λ_{exc}=488 nm and λ_{em}=>505 nm for FITC.

Western blot analysis

Western blot analyses of various components of cells exposed to microgravity and of control cells were carried out following routine protocols. Antibodies against the following human antigens were used for this study: chondroitin sulfate, (Sigma); collagen type I, collagen type III, fibronectin, E-cadherin, transforming growth factor beta$_1$ (TGF-β_1; all Chemicon, Hofheim, Germany), TGF-β receptor type II (TGFBR2; Biomol, Hamburg, Germany), OPN (MPIIIB101, University of Iowa, Hybridoma Bank, USA), and CD44 (Endogen, Woburn, Mass., USA). SDS-polyacrylamide gel electrophoresis and immunoblotting were carried out following routine protocols (Grimm et al. 2001). Blots were quantitated by densitometry (Personal Densitometer 50301, Molecular Dynamics, Krefeld, Germany; Grimm et al. 2001; Shakibaei et al. 1995).

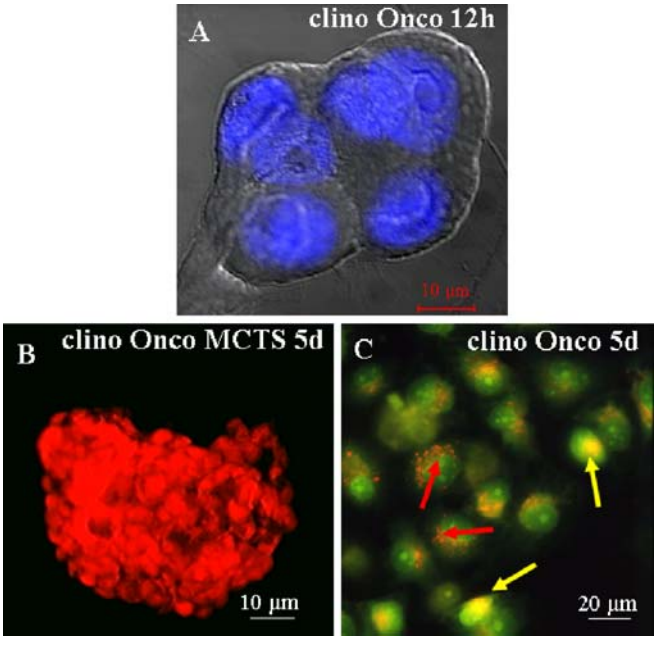

Fig. 1 **a** DAPI staining of a ONCO-DG 1 spheroid after 12 h. **b** Propidium Iodide staining of a 5-day-old ONCO-DG 1 spheroid. No necrotic center is visible after 5 days of culture under conditions of mimicked microgravity. **c** Acridine orange/ethidium bromide viability staining: ONCO-DG1 cells with signs of condensation (phase II: *yellow arrows*) and cell death (phase III: *red arrows*)

RNA isolation

Total RNA from ONCO-DG 1 cells was isolated with the Qiagen Minikit (Hilden, Germany) according to the manufacturer's instructions. The isolated RNA had an $A_{260/280}$ ratio of >1.5. Quality control of the RNA by agarose gel electrophoresis showed no degradation. RNA concentrations were determined spectrophotometrically at 260 nm.

Reverse transcription

Aliquots of 1 μg total RNA was reverse-transcribed in a total volume of 20 μl by using the First Strand cDNA Synthesis Kit (MBI Fermentas) according to the manufacturer's recommendations.

TaqMan polymerase chain reaction

To quantify the expression levels of TGF-β_1 genes, we employed real-time quantitative reverse-transcription ("TaqMan") polymerase chain reaction (RT-PCR). Appropriate primers and fluorogenic probes were designed with Primer Express software. The ABI PRISM 7000 SDS instrument in conjunction with the ABI TaqMan Universal Master Mix (Applied Biosystems, Darmstadt, Germany) was used to perform the assays. A reaction volume of 25 μl was employed with a final concentration of 400 nM for the primers and 200 nM for the probes. PCR conditions were used as recommended by the manufacturer (2 min at 50°C, 10 min at 95°C, 45 cycles of 15 s at 95°C and 1 min at 60°C). Fluorogenic probes were synthesized by TIB Molbiol (Berlin, Germany), and the primers (TGF-β_1, 18S) were obtained from Proligo (Evry Cedex, France).

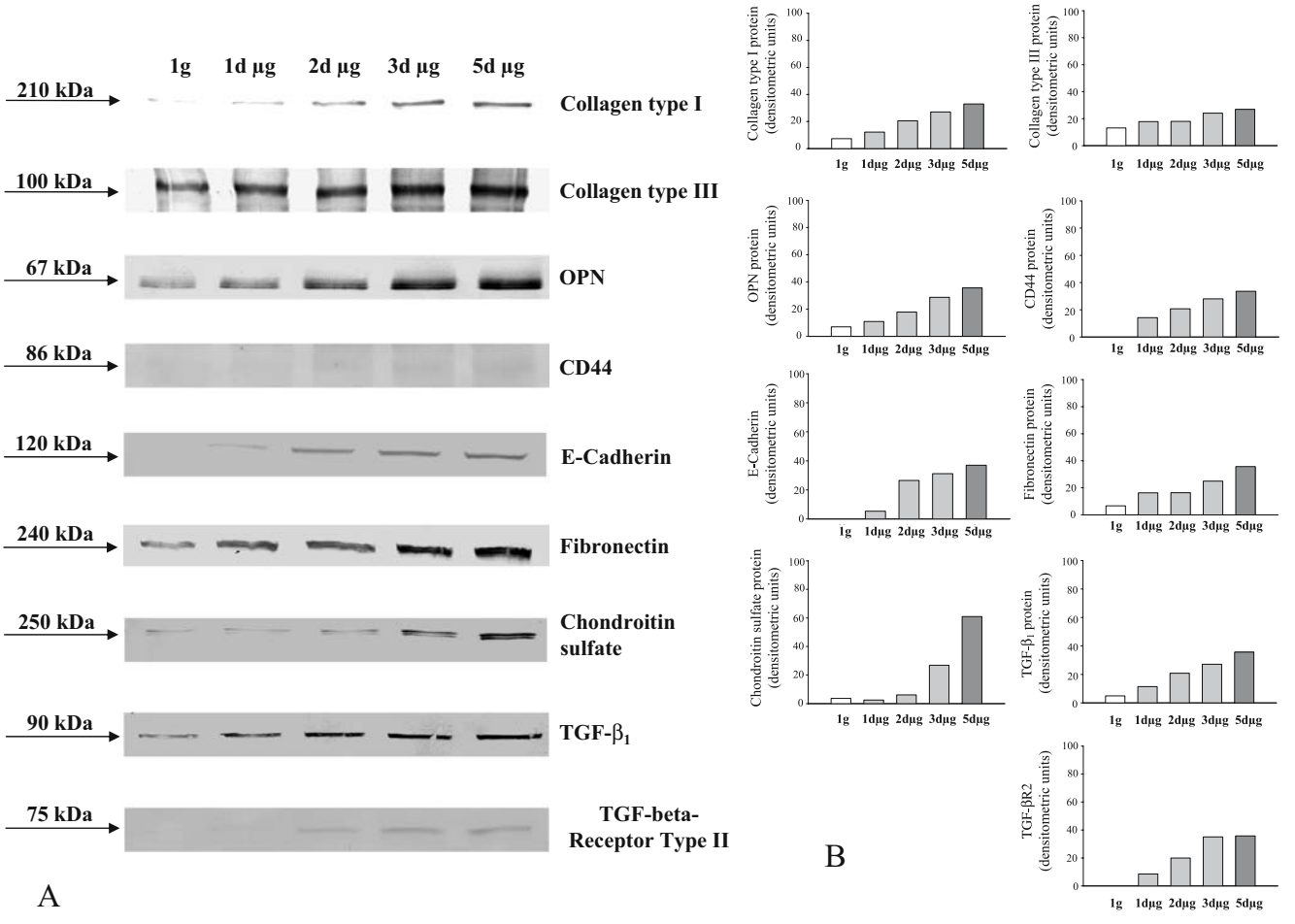

Fig. 2 **a** Western blot analyses of collagen type I and III, osteopontin, CD44, E-cadherin, fibronectin, chondroitin sulfate, TGF-β_1, and TGFBR2 proteins: a time-dependent increase in ECM proteins is detectable in ONCO DG1 cells (*d* day, *μg* microgravity). **b** Densitometric evaluations of the Western blot analyses shown in **a**. **c** Gene expression of TGF-β_1 measured by quantitative TaqMan PCR. **d** Flow cytometric investigation of OPN and CD44 in CGTH-W-1 cells. **e** Fibronectin immunostaining of ONCO-DG 1 static control cells. Fibronectin is not detectable in normal static control cells after 120 h. **f** Fibronectin immunostaining of ONCO-DG 1 cells cultured under mimicked microgravity (120 h). All cells secreted fibronectin

Fig. 2 (continued)

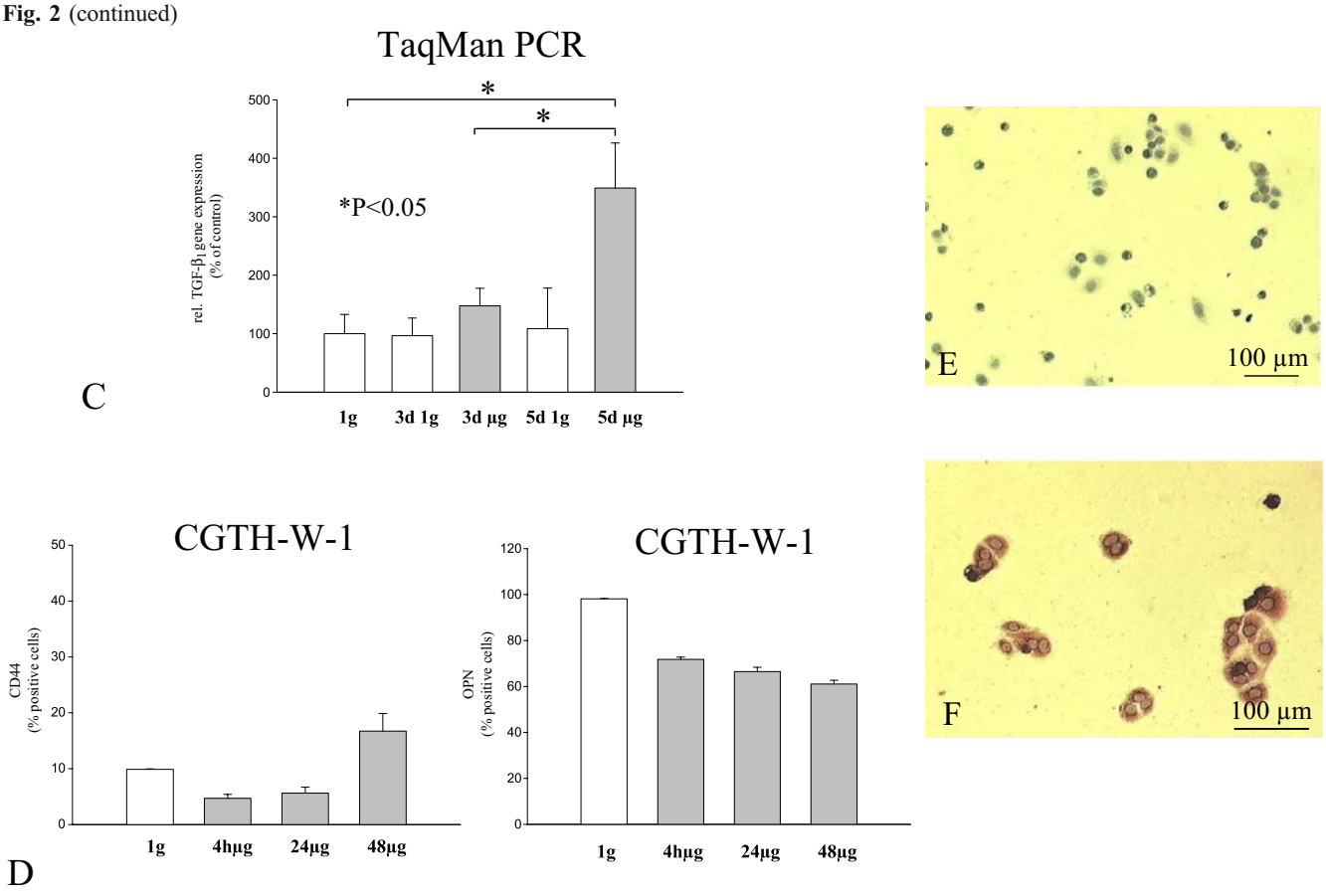

Relative quantitation was performed by using the standard curve method. For each gene, a PCR fragment ("standard") containing the sequence of the TaqMan-system was generated and purified with the QIAquick PCR purification kit (Qiagen). Seven serial 1:10 dilutions of this fragment served as a standard curve that was assayed together with the corresponding unknown samples on each plate. Every sample was measured in triplicate. To normalize our expression data, we used 18S-rRNA as the housekeeping gene.

Flow cytometric analysis of OPN and CD44

In each test, monoclonal antibodies OPN (MPIIIB101, University of Iowa, Hybridoma Bank, USA) and CD44 (Endogen) were added to 10^5 CGTH-W-1 cells that had been prepared and fixed in ethanol (70%) as previously described (Grimm et al. 2002). The cells were incubated for 60 min at room temperature in darkness, washed three times with PBS containing 2% fetal calf serum, incubated for 45 min at room temperature with FITC-conjugated anti-mouse-IgG, and subsequently washed. Finally, the cell suspensions were analyzed with a Facscan flow cytometer (Becton Dickinson, Heidelberg, Germany) equipped with an argon laser. Cells exhibiting fluorescence intensities above the upper limit of the negative control distribution were considered positive.

Statistics

Statistical analysis was performed by using SPSS 11.5.1 (SPSS, Chicago, Ill., USA) with results being expressed as mean±SEM. Comparisons between multiple groups were assessed by one-way ANOVA, including a modified least significant difference (Bonferroni) multiple range test to detect significant differences between two distinct groups; these were further analyzed by using the Mann-Whitney U test. The strength of the relationship between two variables was assessed by calculation of the product moment correlation coefficient (r). Statistical significance was accepted at the level of $P<0.05$.

Results

Long-term culture of ONCO-DG 1 spheroids under conditions of simulated weightlessness

Thyroid cells grown as monolayer cultures were clinorotated. Within the initial 12 h, they detached from their culture flask surfaces and formed three-dimensional spheroids (Fig. 1a). The newly formed spheroids were kept in the rotating clinostat for another 4 days. After 5 days, all spheroids were comparable to the spheroids formed on the first day. During this prolonged stay in simulated weight-

lessness, the spheroids, once formed, enlarged and remained compact, and no signs of decay were observed (Fig. 1b). Acridine orange/ethidium bromide staining of ONCO-DG 1 spheroids revealed that the majority of the cells clinorotated for 12 h remained impermeable to the dyes (Zhou et al. 1997), whereas at 5 days ONCO-DG1 cells exhibited nuclear condensation (phase II) or took up the dyes (phase III; Fig. 1c), indicating cell death.

Analysis of ECM components of ONCO-DG 1 cells by immunoblot techniques

ONCO-DG 1 cells clinorotated for 1, 2, 3, or 5 days were analyzed by immunoblot techniques in order to determine the amounts of type I and III collagen, OPN, fibronectin, and chondroitin sulfate. The levels of collagen type I and III, OPN, and fibronectin were increased compared with 1 *g* control cells after the first 24 h of rotation. After 72 h, chondroitin sulfate had also clearly increased (Fig. 2a). Between the second and the fifth day, the concentrations of all of these ECM components continuously increased in rotated cells compared with 1 *g* cells (Fig. 2b). These results clearly demonstrated that ECM protein levels were (1) upregulated during the first 48 h and (2) produced at elevated rates up to the fifth day of clinorotation. In parallel, CD44 was significantly increased in clinorotated ONCO-DG 1 cells in a time-dependent manner (Fig. 2a). We also investigated malignant CGTH-W-1 thyroid cells derived from a metastasis of a follicular thyroid carcinoma. These cells were all positive for OPN (100%). Interestingly, culture of CGTH-W-1 cells under conditions of zero *g* contained clearly reduced numbers of OPN-positive follicular thyroid carcinoma cells (up to 40% fewer) within 48 h. In parallel, CD44 slightly increased within 48 h of zero *g* (Fig. 2d).

The analysis of E-cadherin expression (the main classical cadherin expressed in epithelial cells) was performed by Western blot analysis. A clear increase in E-cadherin protein was detectable in all clinorotated groups (Fig. 2a,b).

We analyzed the gene expression of TGF-β_1 by quantitative RT-PCR (TaqMan). TGF-β_1 gene expression was 1.5-fold increased after 3 days and further elevated (3.2-fold) after 5 days of clinorotation compared with the corresponding ground controls (Fig. 2c). In addition to the changes in ECM proteins, the levels of TGF-β_1 and of TGF beta receptor type II (TGFBR2) proteins were also elevated when ONCO-DG 1 spheroids were formed within 48 h of clinorotation. As early as 24 h, enhanced TGF-β_1 and TGFBR2 protein levels were found in ONCO-DG 1 cells (Fig. 2a). The difference of TGF-β_1 expression between rotated and non-rotated control cells further increased during the following few days. After 5 days of microgravity exposure, the rotated ONCO-DG 1 cells contained 7.2-fold more TGF-β_1 than the corresponding static control cells.

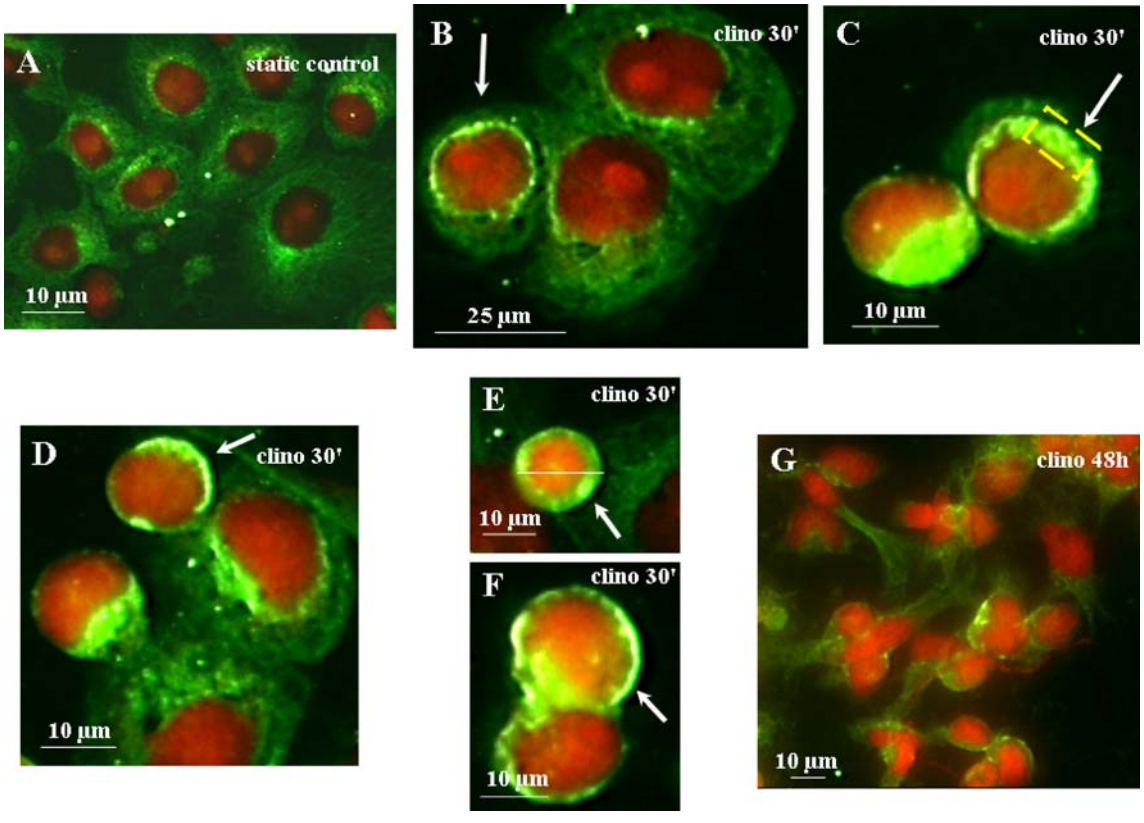

Fig. 3 Immunofluorescence of alpha-tubulin. **a** Static control (1 *g*) cells. Microtubules radiated from a microtubule organizing center to the plasma membrane. **b–f** 30 min clinorotation. Microtubules were disorganized, the radial disposition was lost, and tubulin was found around the nucleus (*arrows*). Nuclei were counterstained with propidium iodide. **c** Compact alpha-tubulin accumulation near the nucleus (*boxed area*). **g** Microtubular restoration was observed after 48 h

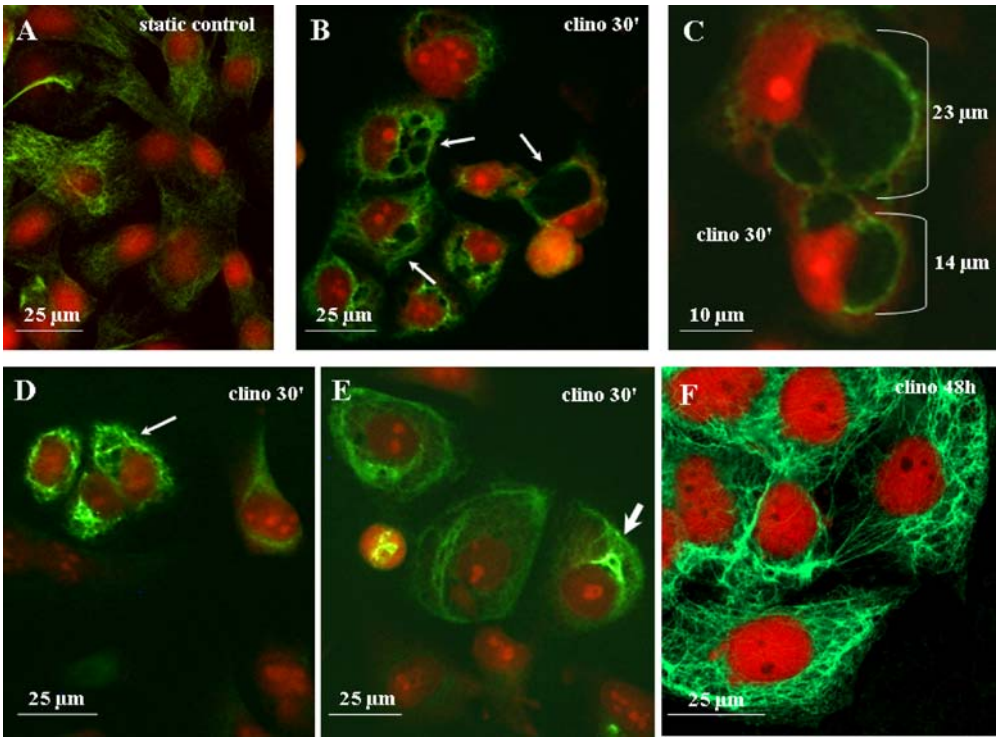

Fig. 4 Immunofluorescence of anti-cytokeratin. **a** Normal distribution of cytokeratin filaments in ONCO-DG 1 static control cells. **b–e** Clinorotation for 30 min. **b**, **c** Looser meshes of the intermediate filament network are visible (*arrows*). **d**, **e** Intermediate filaments become thicker and coalesce (*arrow*). **f** After 48 h of clinorotation, the filaments become thicker, and all ONCO-DG 1 cells are cytokeratin-positive

The synthesis of the fibronectin proteins was increased in all microgravity-treated cells. Immunocytochemical staining of ONCO-DG 1 cells showed that all cells cultured for 120 h under conditions of simulated microgravity (Fig. 2f) could be stained by anti-fibronectin antibodies, whereas cells of the static control were not stained at all (Fig. 2e).

Alterations of the cytoskeleton

Our data clearly showed that, after 30 min under simulated weightlessness, the cytoskeleton had disintegrated. Microtubules (alpha-tubulin), which radiated from an organizing center to the cellular membrane in a static controls at 1 *g* (Fig. 3a), lost their radial arrays and gathered around the

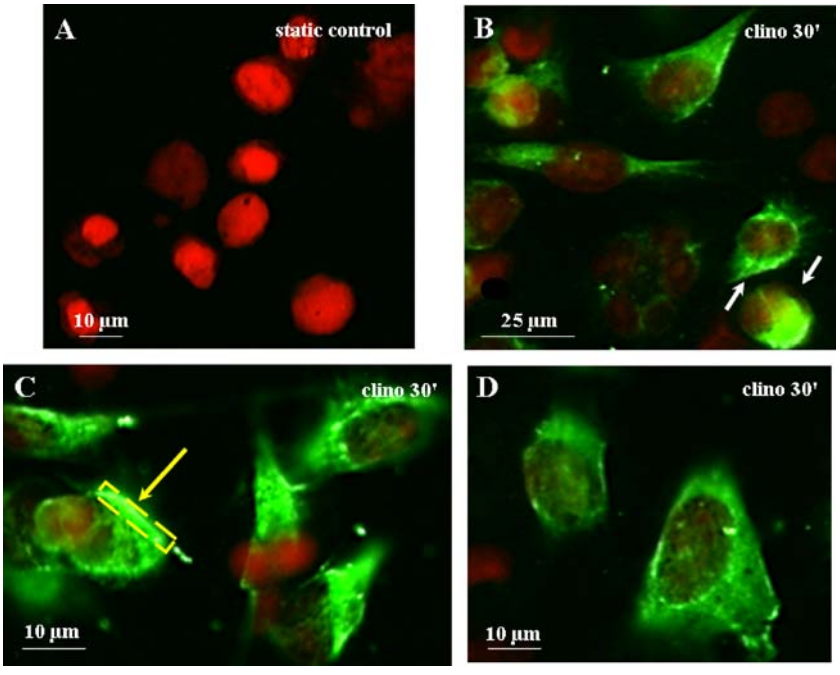

Fig. 5 Immunofluorescence of vimentin. **a** The intermediate filament component vimentin is not detectable in ONCO-DG 1 static control cells. **b–d** Clinorotation for 30 min. The vimentin network is detectable in the form of dense aggregates (*arrow*) closely associated with the nucleus (*boxed area* in **c**)

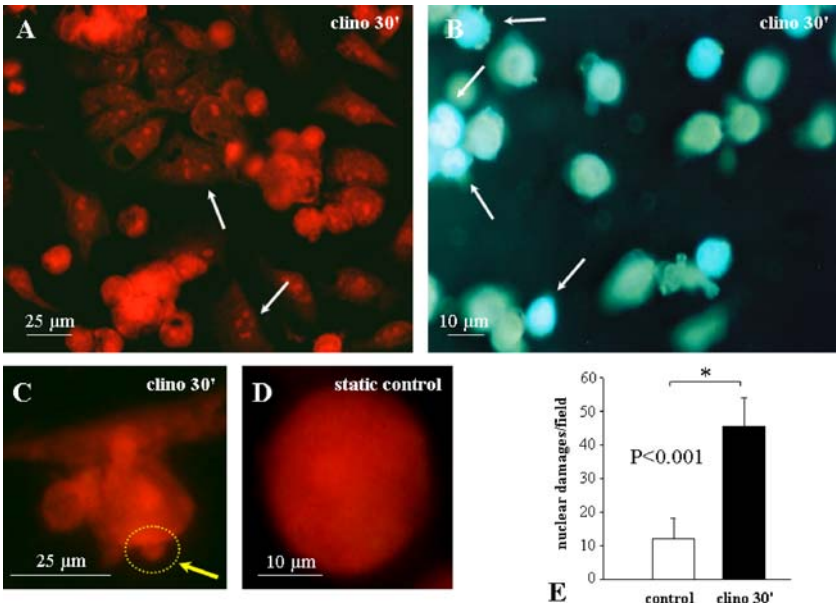

Fig. 6 **a** Propidium iodide staining after 30 min simulated microgravity (*arrows* activated nuclei). **b** DAPI staining of nuclei (*arrows* damaged nuclei). After 30 min at zero *g*, numerous nuclei underwent the classical morphological alterations (chromatin condensation, nuclear fragmentation, apoptotic bodies) that lead to programmed cell death. **c** More membrane blebbing (*arrow*, *dotted circle*) is detectable than in static control cells. **d** Normal nucleus of static control cells. **e** Image analysis of ONCO-DG 1 cells demonstrating a four-fold increase in nuclear damage

nucleus after 30 min clinorotation (Fig. 3b–f). The cell shape deteriorated, and nuclei showed chromatin condensation and blebbing. However, after 48 h, partial restoration of the natural structures of microtubules could be observed (Fig. 3g).

Similarly, in the static ground control cells, cytokeratin networks displayed characteristic patterns depending on their intracellular localization (Fig. 4a). After 30 min in microgravity, the meshes of the network had been loosened (Fig. 4b–e). After 48 h of clinorotation, the intermediate filament network for cytokeratin reorganized (Fig. 4f). The intermediate filament component vimentin, which was not detectable throughout the cytoplasm of the papillary thyroid carcinoma cells in the 1 *g* static controls (Fig. 5a), had considerably increased after 30 min of clinorotation (Fig. 5b–d). Disruptions in the network were detected. Vimentin was gathered in a dense ring around the nucleus.

Early changes of nuclear morphology

After 30 min of culture of papillary thyroid carcinoma cells under simulated microgravity, considerable alterations of the nuclear shape had been induced. Blebbing of the nuclear membrane was detectable, nucleoli appeared, and chromatin condensation was visible. Propidium iodide and DAPI staining revealed a significant increase in nuclear alterations, which could be quantified by image analyses (Fig. 6).

Discussion

This is the first study of the long-term effects of simulated weightlessness on human papillary thyroid carcinoma cells. Papillary thyroid carcinoma cells clinorotated for up to 5 days on a random-positioning machine survived by forming MCS.

Interpretation of data from experiments carried out under simulated microgravity requires that stress-associated alterations with clinorotation, including experiment-induced stress and the effects of the clinostat room, can be distinguished. We addressed these factors by using static controls (ground controls in the clinostat room) to ensure that the observed alterations were induced exclusively by weightlessness. All samples were identically treated before the start of the experiment and randomized for clinorotation or for culturing at 1 *g*. Formation of spheroids of various human tumor cell lines and normal cells was also demonstrated by using a high-aspect ratio vessel in a NASA rotary cell culture system to simulate microgravity (Grimm et al. 1995).

Using clinorotation, we observed that the ECM responded to microgravity in a sensitive fashion. This study showed, for the first time, that enhanced production rates of ECM proteins lasted for at least 5 days in human papillary thyroid carcinoma cells. After 24 h, we detected a clear increase in structural proteins, such as type I and III collagen and fibronectin. The greatest amount of these proteins was measured at day 5. Interestingly, we recorded a time-dependent increase in OPN, a secreted adhesive glycoprotein that is significantly overexpressed in a variety of carcinomas from the breast, lung, and ovary. Whereas constitutive expression of OPN exists in several cell types, induced expression has been detected in T-lymphocytes, epidermal cells, bone cells, macrophages, and tumor cells in remodeling processes such as inflammation, ischemia reperfusion, bone resorption, and tumor progression. Recently, substantial evidence has linked OPN with the regulation of metastatic spread by tumor cells. Moreover, OPN is involved in a number of physiological and pathological events, including angiogenesis, apoptosis, inflammation, and wound healing (Schnee and Hsueh 2000). It has been shown to bind covalently to fibronectin via transglutaminase-catalyzed cross-linking. As an adhesion protein, it has been also proposed to bind to calcium and to collagen (Ingram et al.

1997). This interaction with fibronectin and collagen indicates its importance in ECM organization (Standal et al. 2004). In addition, soluble OPN inhibits apoptosis of adherent human umbilical vein endothelial cells incubated in medium lacking critical growth factors and cytokines. In a dose-dependent manner, OPN reduces the formation of apoptotic bodies and suppresses DNA fragmentation. These data suggest that one function of OPN in homeostatic processes is to facilitate the survival of stressed endothelial cells, possibly by occupying unligated integrins and suppressing integrin-mediated death (Schnee and Hsueh 2000). The increase in OPN detected in ONCO-DG 1 cells cultured in simulated weightlessness may protect non-apoptotic human thyroid carcinoma cells from programmed cell death. In parallel, we have also measured an increase in CD44 in ONCO-DG 1 cells cultured under zero *g*. Guarino et al. (2005) have recently shown that the prevalence and intensity of OPN staining seems significantly correlated with the presence of metastases in papillary thyroid carcinomas. We have detected 100% OPN-positive CGTH-W-1 cells (established from the metastasis of a follicular carcinoma) cultured under normal conditions (1 *g*). This finding supports the hypothesis that OPN also plays a role in the enhancement of follicular thyroid carcinoma cell invasiveness and correlates with poor prognosis. Clinorotation clearly reduces OPN in CGTH-W-1 cells. Future studies will be performed to explain this finding. Furthermore, CD44 receptor is increased in clinorotated CGTH-W-1 samples compared with static ground controls.

Concomitantly, chondroitin sulfate protein increases in a time-dependent manner. Only scant chondroitin sulfate has been detected in static control cells. Little is known about the function of chondroitin sulfate in thyroid cancer spheroids. We have previously demonstrated chondroitin sulfate in follicular thyroid carcinoma spheroids formed under zero *g* (Grimm et al. 2002). Kawata et al. (1991) have detected neural rosette formation within spheroids of the teratocarcinoma cell line PA-1/NR. This rosette formation in the spheroids is accompanied by deposition of chondroitin sulfate proteoglycans (Mukherjee et al. 1995). Chondroitin sulfate is known to inhibit the adhesion of cells to ECM proteins, and this inhibition is mediated through cell-specific receptors, resulting in the cessation of cell spreading (Khan et al. 2002). Its detection in the spheroids formed under zero *g* conditions indicates a role for chondroitin sulfate in the development and maintenance of spheroid structure.

Like the ECM proteins, TGF-β_1 and TGFBR2 are also upregulated and produced at an elevated rate under microgravity. TGF-β_1 is known to enhance the production of various structural proteins (Kawata et al. 1991). It is tempting, therefore, to assume that TGF-β_1 plays a role in microgravity-induced enhancement of ECM production in thyroid cells (Ernst et al. 1995). ONCO-DG 1 cells show enhanced TGF-β_1 concentrations after 24 h and significantly enhanced ECM proteins after 48 h. TGF-β_1 is known to promot the disruption of follicles, cell spreading, migration, and confluency by a mechanism that does not involve cell proliferation in porcine thyroid cells; it also induces the formation of a tight monolayer and domes (Claisse et al. 1999). It also may play a role in the aggregation and formation of MCS under conditions of weightlessness in our experimental setting.

The ONCO-DG 1 cell line, an oxyphilic papillary thyroid carcinoma cell line (Grimm et al. 1992), is negative for E-cadherin. Loss of E-cadherin, a Ca^{2+}-dependent cell adhesion molecule required for normal epithelial function, has been attributed to a pathogenetic role in tumor invasion. Brabant et al. (1993) have shown that, in anaplastic thyroid carcinomas, E-cadherin expression is low or lacking, whereas in papillary carcinomas, E-cadherin mRNA levels vary from nearly normal to highly reduced, which roughly correlates with the overall immunofluorescence intensity; their data suggest that, in human thyroid malignancies, both gene expression and post-transcriptional control of E-cadherin is impaired. Here, we have demonstrated, for the first time, that E-cadherin is elevated during the culture of ONCO-DG 1 cells under simulated weightlessness. ONCO-DG 1 cells grow in the form of three-dimensional MCS in weightlessness. This finding indicates the putative protection from programmed cell death in human papillary thyroid carcinoma cells.

Here, we report that structural changes occur to the cytoskeleton of papillary thyroid carcinoma cells after 30 min of cell culture under conditions of simulated weightlessness. Normally, the ONCO-DG 1 cell line only displays a few vimentin-positive cells. The amount of vimentin-positive cells increases after 30 min under microgravity. Monolayer cultured ONCO-DG 1 cells exhibit morphological alterations as early as 30 min under mimicked zero *g*. The intermediate filament network, responsible for the shape and positioning of the nucleus, is disorganized, and the microtubules, which are responsible for cell division, lose their radial disposition. The papillary thyroid carcinoma cells reorganize their cytoskeleton after 48 h.

Moreover, abnormalities in actin stress fibres in osteoblasts and changes of microtubulin in Jurkat cells flown on the space shuttle have previously been reported (Uva et al. 2002). These abnormalities may arise because proper tubulin association is gravity-dependent (Uva et al. 2002) and may be the reason that mitochondria abandon their natural order of localization (Baghdassarian et al. 1993).

The technique of clinorotation has been applied in gravitational biology since 1965 in order to investigate possible effects of microgravity and to develop experimental systems and hypotheses concerning gravitational cell biology (O'Connor et al. 1997). Recently, the role of clinostat studies have become more and more important in producing organ-like cell aggregates and in the study of apoptosis (Khaoustov et al. 1999). The random-positioning machine (clinostat) is an important tool for studying conditions of weightlessness on earth. Experiments can be repeated, which is not possible in spaceflight experiments. Here, we have demonstrated, for the first time, that microgravity rapidly alters the cytoskeleton of papillary thyroid carcinoma cells. In addition, we have performed long-term experiments by clinostat rotation and revealed the growth of multicellular tumor spheroids with increasing amounts of ECM proteins.

Acknowledgements We thank Dr. Chris Talsness for language editing. We are grateful to Roderick MacLeod for providing the CGTH-W-1 cell line.

References

Adams JC, Watt FM (1993) Regulation of development and differentiation by the extracellular matrix. Development 117: 1183–1198

Baghdassarian D, Torudel-Bauffe D, Gavaret JM, Pierre M (1993) Effects of transforming growth factor-beta-1 on the extracellular matrix and cytoskeleton of cultured astrocytes. Glia 7:193–202

Brabant G, Hoang-Vu C, Cetin Y, Dralle H, Scheumann G, Molne J, Hansson G, Jansson S, Ericson LE, Nilsson M (1993) E-cadherin: a differentiation marker in thyroid malignancies. Cancer Res 53:4987–4993

Claisse D, Martiny I, Chaqour B, Wegrowski Y, Petitfrere E, Schneider C, Haye B, Bellon G (1999) Influence of transforming growth factor beta1 (TGF-beta1) on the behaviour of porcine thyroid epithelial cells in primary culture through thrombospondin-1 synthesis. J Cell Sci 112:1405–1416

Cogoli M (1992) The fast rotating clinostat: a history of its use in gravitational biology and a comparison of ground-based and flight experiment results. ASGSB Bull 5:59–67

Ernst H, Zanin MK, Everman D, Hoffman S (1995) Receptor-mediated adhesive and anti-adhesive functions of chondroitin sulfate proteoglycan preparations from embryonic chicken brain. J Cell Sci 108:3807–3816

Grimm D, Hofstädter F, Bauer J, Spruss T, Steinbach P, Bernhardt G, Menze R (1992) Establishment and characterization of a human papillary thyroid carcinoma cell line with oxyphilic differentiation (ONCO-DG 1). Virchows Arch 62:97–104

Grimm D, Bauer J, Kromer E, Steinbach P, Riegger G, Hofstadter F (1995) Human follicular and papillary thyroid carcinoma cells interact differently with human venous endothelial cells. Thyroid 5:155–164

Grimm D, Bauer J, Hofstädter F, Riegger GAJ, Kromer EP (1997) Characteristics of multicellular spheroids formed by primary cultures of human thyroid tumor cells. Thyroid 7:859–865

Grimm D, Huber M, Jabusch HC, Shakibaei M, Fredersdorf S, Paul M, Riegger GA, Kromer EP (2001) Extracellular matrix proteins in cardiac fibroblasts derived from rat hearts with chronic pressure overload: effects of β-receptor blockade. J Mol Cell Cardiol 33:487–501

Grimm D, Bauer J, Kossmehl P, Shakibaei M, Schönberger J, Pickenhahn H, Schulze-Tanzil G, Vetter R, Eilles C, Paul M, Cogoli A (2002) Simulated microgravity alters differentiation and increases apoptosis in human follicular thyroid carcinoma cells. FASEB J 16:U55–U81

Guarino V, Faviana P, Salvatore G, Castellone MD, Cirafici AM, De Falco V, Celetti A, Giannini R, Basolo F, Melillo RM, Santoro M (2005) Osteopontin is overexpressed in human papillary thyroid carcinomas and enhances thyroid carcinoma cell invasiveness. J Clin Endocrinol Metab 90:5270–5278

Hagios C, Lochter A, Bissell MJ (1998) Tissue architecture: the ultimate regulator of epithelial function? Philos Trans R Soc Lond Biol 353:857–870

Hoson T, Kamisaka S, Masuda Y, Yamashita M (1992) Changes in plant growth processes under microgravity conditions simulated by a three-dimensional clinostat. Bot Mag 105:53–70

Hughes-Fulford M, Lewis ML (1996) Effects of microgravity on osteoblast growth activation. Exp Cell Res 224:103–109

Ingram M, Techy GB, Saroufeem R, Yazan O, Narayan KS, Goodwin TJ, Spaulding GF (1997) Three-dimensional growth patterns of various human tumor cell lines in simulated microgravity of a NASA bioreactor. In Vitro Cell Dev Biol Anim 33:459–466

Kawata M, Sekiya S, Kera K, Kimura H, Takamizawa H (1991) Neural rosette formation within in vitro spheroids of a clonal human teratocarcinoma cell line, PA-1/NR: role of extracellular matrix components in the morphogenesis. Cancer Res 51: 2655–2669

Khan SA, Lopez-Chua CA, Zhang J, Fisher LW, Sorensen ES, Denhardt DT (2002) Soluble osteopontin inhibits apoptosis of adherent endothelial cells deprived of growth factors. J Cell Biochem 85:728–736

Khaoustov VI, Darlington GJ, Soriano HE, Krishnan B, Risin D, Pellis NR, Yoffe B (1999) Induction of three-dimensional assembly of human liver cells by simulated microgravity. In Vitro Cell Dev Biol Anim 35:501–550

Kossmehl P, Shakibaei M, Cogoli A, Infanger M, Curcio F, Schoenberger J, Eilles C, Bauer J, Pickenhahn H, Schulze-Tanzil G, Paul M, Grimm D (2003) Weightlessness induced apoptosis in normal thyroid and carcinoma cells. Endocrinology 144:4172–4179

Lelievre SA, Weaver VM, Nickerson JA, Larabell CA, Bhaumik A, Petersen OW, Bissell MJ (1998) Tissue phenotype depends on reciprocal interactions between the extracellular matrix and the structural organization of the nucleus. Proc Natl Acad Sci USA 95:14711–14716

Lewis ML, Reynolds JL, Cubano LA, Hatton JP, Lawless BD, Piepmeier EH (1998) Spaceflight alters microtubules and increases apoptosis in human lymphocytes (Jurkat). FASEB J 12:1007–1018

Lewis ML, Cubano LA, Zhao BT, Dinh HK, Pabalan JG, Piepmeier EH, Bowman PD (2001) cDNA microarray reveals altered cytoskeletal gene expression in space-flown leukemic T lymphocytes (Jurkat). FASEB J 15:U277–U279

Lin JD, Chao TC, Weng HF, Huang HS, Ho YS (1996) Establishment of xenografts and cell lines from well-differentiated human thyroid carcinoma. J Surg Oncol 63:112–118

Maccarrone M, Battista N, Meloni M, Bari M, Galleri G, Pippia P, Cogoli A, Finazzi-Agro A (2003) Creating conditions similar to those that occur during exposure of cells to microgravity induces apoptosis in human lymphocytes by 5-lipoxygenase-mediated mitochondrial uncoupling and cytochrome c release. J Leukoc Biol 73:472–481

Margolis L, Hatfill S, Chuaqui R, Vocke C, Emmert-Buck M, Linehan WM, Duray PH (1999) Long term organ culture of human prostate tissue in a NASA-designed rotating wall bioreactor. J Urol 161:290–297

Martin A, Zhou A, Gordon RE, Henderson SC, Schwartz AE, Friedman EW, Davies TF (2000) Thyroid organoid formation in simulated microgravity: influence of keratinocyte growth factor. Thyroid 10:481–487

Merker HJ (1994) Morphology of the basement membrane. Microsc Res Tech 28:95–124

Mukherjee BB, Nemir M, Beninati S, Cordella-Miele E, Singh K, Chackalaparampil I, Shanmugam V, DeVouge MW, Mukherjee AB (1995) Interaction of osteopontin with fibronectin and other extracellular matrix molecules. Ann N Y Acad Sci 760:201–212

Nicogossian AE, Huntoon CL, Pool S (1989) In: Nicogossian AE (ed) Space physiology and medicine, 2nd edn. Lea and Febiger, Philadelphia

O'Connor KC, Enmon RM, Dotson RS, Primavera AC, Clejan S (1997) Characterization of autocrine growth factors, their receptors and extracellular matrix present in three-dimensional cultures of DU 145 human prostate carcinoma cells grown in simulated microgravity. Tissue Eng 3:161–171

Roskelley CD, Desprez PY, Bissell MJ (1994) Extracellular matrix-dependent tissue-specific gene expression in mammary epithelial cells requires both physical and biochemical signal transduction. Proc Natl Acad Sci USA 91:12378–12382

Schatten H, Lewis ML, Chakrabarti A (2001) Spaceflight and clinorotation cause cytoskeleton and mitochondria changes and increases in apoptosis in cultured cells. Acta Astronaut 49: 399–418

Schnee JM, Hsueh WA (2000) Angiotensin II, adhesion, and cardiac fibrosis. Cardiovasc Res 46:264–268

Shakibaei M, Zimmermann B, Merker HJ (1995) Changes in integrin expression during chondrogenesis in vitro: an immunomorphological study. J Histochem Cytochem 43:1061–1069

Standal T, Borset M, Sundan A (2004) Role of osteopontin in adhesion, migration, cell survival and bone remodeling. Exp Oncol 26:179–184

Uva BM, Masini MA, Sturla M, Bruzzone F, Giuliani M, Tagliafierro G, Strollo F (2002) Microgravity-induced apoptosis in cultured glial cells. Eur J Histochem 46:209–214

Vassy J, Portet S, Beil M, Millot G, Fauvel-Lafeve F, Karniguian A, Gasset G, Irinopoulou T, Calvo F, Rigaut JP, Schoevaert D (2001) The effect of weightlessness on cytoskeleton architecture and proliferation of human breast cancer cell line MCF-7. FASEB J 15:1104–1106

White RJ, Averner M (2001) Humans in space. Nature 409:1115–1118

Yurchenco PD, O'Rear JJ (1994) Basal lamina assembly. Curr Opin Cell Biol 6:674–681

Zhou P, Qian L, Kozopas KM, Craig RW (1997) Mcl-1, a Bcl-2 family member, delays the death of hematopoietic cells under a variety of apoptosis-inducing conditions. Blood 89:630–643